

QikProp 2.5

Technical Notes

Copyright © 2006 Schrödinger, LLC. All rights reserved. CombiGlide, Epik, Glide, Impact, Jaguar, Liaison, LigPrep, Maestro, Phase, Prime, QikProp, QikFit, QikSim, QSite, SiteMap, and Strike are trademarks of Schrödinger, LLC.

Schrödinger and MacroModel are registered trademarks of Schrödinger, LLC.

To the maximum extent permitted by applicable law, this publication is provided “as is” without warranty of any kind. This publication may contain trademarks of other companies.

Please note that any third party programs (“Third Party Programs”) or third party Web sites (“Linked Sites”) referred to in this document may be subject to third party license agreements and fees. Schrödinger, LLC and its affiliates have no responsibility or liability, directly or indirectly, for the Third Party Programs or for the Linked Sites or for any damage or loss alleged to be caused by or in connection with use of or reliance thereon. Any warranties that we make regarding our own products and services do not apply to the Third Party Programs or Linked Sites, or to the interaction between, or interoperability of, our products and services and the Third Party Programs. Referrals and links to Third Party Programs and Linked Sites do not constitute an endorsement of such Third Party Programs or Linked Sites.

April 2006

Contents

Chapter 1: Quality of Results	1
1.1 Test Set Results	1
1.2 Accuracy Issues	5
1.3 Conformation Dependence of Results	6
Chapter 2: Statistical Analysis and Plots of Results	9
2.1 Octanol-Water Partition Coefficient, log P(o/w)	10
2.2 Aqueous Solubility, log S	11
2.3 Brain-Blood Partition Coefficient, log BB	12
2.4 Binding Affinity for Human Serum Albumin, log K _h sa	13
2.5 Free Energies of Hydration, $-2.3RT \log L_w$	14
2.6 Apparent Caco-2 cell permeability, log PCaco (Combined Data Sets)	15
2.7 MDCK Cell Permeability, log PMDCK (Affymax Data)	16
2.8 Blockage of Mammalian HERG K ⁺ Channels, log IC ₅₀	17
2.9 Skin Permeability, log K _p	18
References	21

Quality of Results

Experimental results for more than 710 compounds including about 500 drugs and related heterocycles were used in developing QikProp. The following table summarizes the fits for QikProp 2.2.

Table 1.1. Statistics on QikProp 2.2 Fits to Experimental Data

Property	N	r ²	RMS error	MW range
polarizability (Å ³)	78	0.97	1.05	20–200
log P (hexadecane/gas)	392	0.93	0.37	20–200
log P (octanol/gas)	117	0.91	0.61	20–250
log P (water/gas)	421	0.93	0.58	20–250
log P (octanol/water)	448	0.93	0.50	20–735
log S (water/solid)	389	0.91	0.63	20–823
log K _h sa (serum protein binding)	90	0.82	0.25	130–765
log IC ₅₀ for HERG blockage	47	0.76	0.80	275–750
log BB (brain/blood)	104	0.80	0.35	20–525
log P Caco-2	126	0.72	0.61	60–520
log P MDCK	52	0.73	0.57	130–430
log K _p (skin permeability)	58	0.78	0.68	20–600

In the QikProp output file for the log P (octanol/water), log S and log BB output, if the value for a utilized descriptor exceeds the range for the experimental training set, it is flagged. Otherwise, the molecular weight ranges above indicate the domain of validated applicability of the regression equations.

1.1 Test Set Results

The following tables illustrate results for test sets of molecules that were not in the QikProp 2.2 training set. The 3D structures were obtained directly from SciFinder, then to gauge the effect

of optimization, they were optimized with the BOSS program using the OPLS-AA force field and CM1P charges. Both sets of structures were processed by QikProp 2.2

Table 1.2. Log S results for a test set of molecules.

Molecule	MW	exptl log S	QPlogS^a	QPlogS^b
N-methylmorpholine	101.1	1.00	1.85	1.66
2,5-dimethylpiperazine	114.2	0.49	1.47	1.36
Isoniazid	137.1	0.01	-0.79	-0.85
3,3-dimethyl-1-butanol	102.2	-0.50	-0.81	-0.88
3-methyl-3-hexanol	116.2	-1.00	-1.99	-1.53
bis-(2-chloroethyl) sulfone	191.1	-1.50	-1.48	-1.42
Minoxidil	209.3	-1.98	-2.07	-1.92
2,4-D	221.0	-2.51	-2.21	-2.78
Heptabarbital	250.3	-3.00	-2.29	-2.30
Sulfadiazine	250.3	-3.51	-2.08	-2.06
Terbutyrne	241.4	-4.00	-2.89	-3.57
1,2,4-tribromobenzene	314.8	-4.50	-4.00	-4.05
Quinonamid	318.5	-5.03	-3.34	-3.89
Benfluralin	335.3	-5.53	-4.08	-4.49
Fluoranthene	202.3	-6.00	-6.44	-6.61
o,p'-DDD	320.0	-6.51	-6.53	-6.90
7,12-dimethylbenz(a)anthracene	256.3	-7.02	-6.40	-6.90
2,2',3,4,6-PCB	326.4	-7.43	-8.04	-7.71
benzo(j)fluoranthene	252.3	-8.00	-8.24	-8.63
2,2',4,4',5,5'-PCB	360.9	-8.56	-10.75	-8.50
q ²			0.89	0.95
RMS			1.01	0.70
Average error			0.77	0.55

a. Using structures from SciFinder.

b. Using optimized structures.

Table 1.3. Log $P_{o/w}$ results for a test set of molecules.

Molecule	MW	exptl log $P_{o/w}$	QPlogPo/w ^a	QPlogPo/w ^b
Isoniazid	137.1	-0.70	-0.24	-0.04
Nicotinamide	122.1	-0.37	-0.13	-0.20
N-methylmorpholine	101.1	-0.33	-0.65	-0.52
Sulfadiazine	250.3	-0.09	-0.06	0.02
Pyrazole	68.1	0.26	0.21	0.20
Sulfamethiazole	270.3	0.54	-0.40	-0.39
Minoxidil	209.3	1.24	1.00	1.13
Heptabarbital	250.3	2.03	0.82	0.86
2,4-D	221.0	2.81	2.03	2.27
Ethisterone	312.5	3.11	3.78	4.35
Pericyazine	365.5	3.52	3.19	3.34
Terbutyrne	241.4	3.74	2.52	2.82
Captafol	349.1	3.80	2.83	3.13
Doxepin	279.4	4.29	3.41	4.00
Biquinoline	256.3	4.31	4.25	4.35
Prochlorperazine	373.9	4.88	3.82	3.79
Fluoranthene	202.3	5.16	5.03	5.13
Benfluralin	335.3	5.29	3.99	4.76
Amitraz	293.4	5.50	5.60	5.86
7,12-dimethylbenz(a)anthracene	256.3	5.80	5.28	5.63
q ²			0.86	0.92
Rms			0.84	0.65
ave. error			0.63	0.47

a. Using structures from SciFinder.

b. Using optimized structures.

Some of the structures from the test sets are shown below.

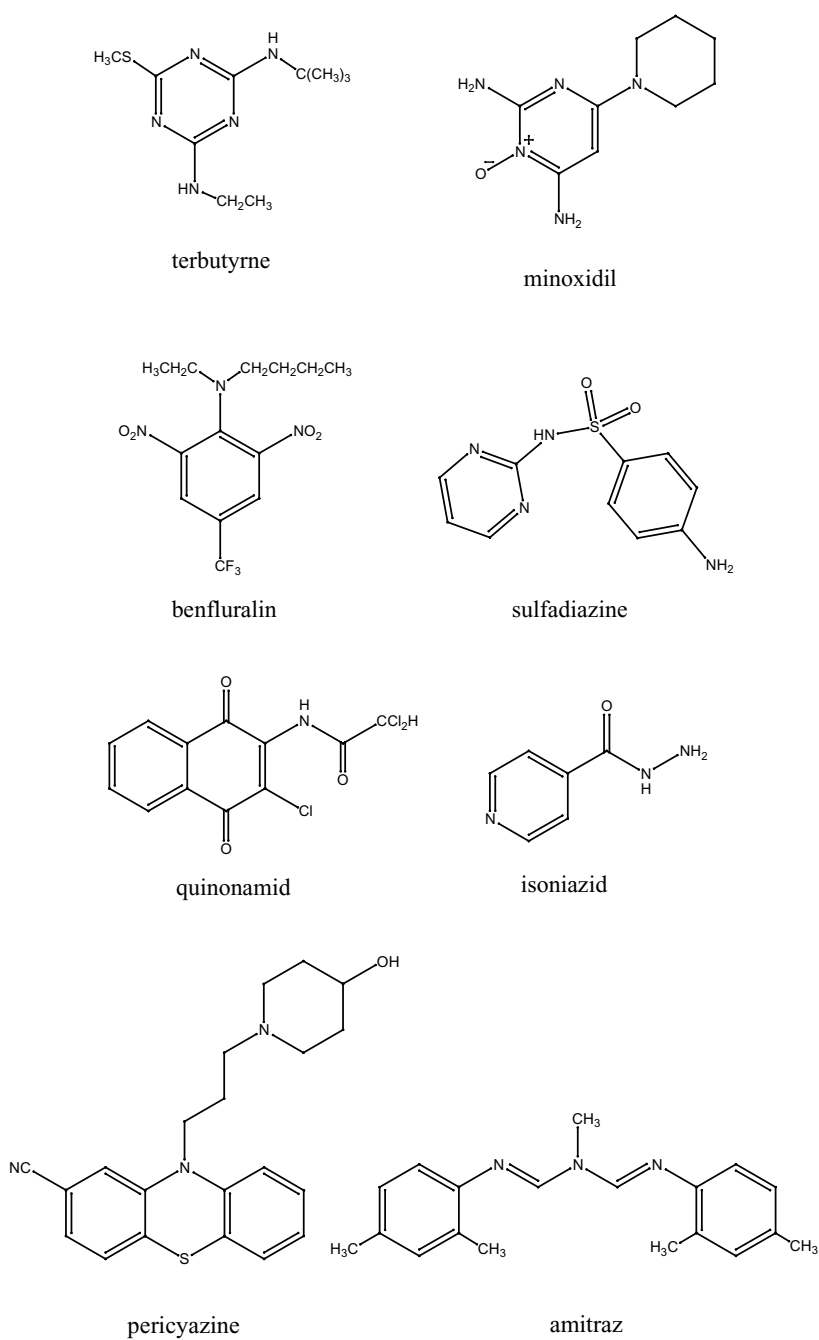


Figure 1.1. Selected structures from the test set.

1.2 Accuracy Issues

QikProp predictions are performed for specific conditions (pH 7, for one), and comparison of the results with experiment must take into account any differences in those conditions. The following issues can affect the accuracy of the comparison:

- active vs passive transport mechanisms
- efflux pump mechanisms
- smaller number of compounds in the training sets
- different experimental conditions than that used in the regression
- noise in experimental data due to inherent complexity of chemical systems interacting with biological systems

The biggest discrepancies are for PCaco predictions, owing to these issues. Values for log BB are less problematic. The QikProp fit for log BB is very good—at the noise level of the data—but there are a few outliers such as oxazepam and tiotidine that are not fitted by any regression method.

Obtaining reliable experimental data for log S requires pure, non-hydrated, no-salt crystals in equilibrium with a saturated aqueous solution. This condition is often difficult to achieve, so it is important to check the experiments as well as the QikProp predictions.

Comparisons must take into account the protonation state of molecules at physiological pH. For example, compounds that contain a tertiary amine are protonated at that pH, and log P measurements must be performed at pH 11, and corrected to pH 7.

Experimental log P values (such as log Po/w) for amino acids, which have a saturated amine and a carboxylic acid, are affected by the protonation state. Though the Hansch * value is supposed to correspond to the un-ionized state, there is no pH at which either the amine is not protonated or the COOH deprotonated or both. The Hansch * values in these cases correspond to a pseudo log D at pH 7, at which pH the acid group is ionized, but the amino group's protonation has been corrected for. The data in [Table 1.4](#) clearly show the problem.

*Table 1.4. Hansch * values for selected molecules*

Molecule	* Value	Molecule	* Value
ethanol HOCH ₂ CH ₃	-0.31	hydroxyacetic acid HOCH ₂ COOH	-1.11
ethylamine H ₂ NCH ₂ CH ₃	-0.13	aminoacetic acid (glycine) H ₂ NCH ₂ COOH	-3.21
difference	-0.18	difference	+2.10

The difference for an alcohol and an un-ionized amine should be -0.18 , but for the two molecules that have an acid group, the difference is $+2.10$. If the acid in both cases was un-ionized, the difference should still be -0.18 . In fact, the value of -1.11 is for the un-ionized acid, but the value of -3.21 is for the ionized acid. The discrepancy of 2.28 is exactly what is expected for the un-ionized acid, i.e.

$$\text{pH } 7.0 - \text{pKa of RCOOH } (4.8) = 2.2$$

The true un-ionized Hansch * value for glycine should be about -1.0 ; QikProp 1.5 gives -0.96 .

The above issues do not apply to peptides in general, which may be capped. QikProp 1.5 agrees with Hansch * values for capped peptides, as illustrated in [Table 1.5](#).

*Table 1.5. Comparison of Hansch * values and QikProp predictions for capped peptides.*

Peptide	Hansch * Value	QikProp 1.5
AcMetValNH ₂	-0.28	-0.19
Ac(Ala) ₃ NHtBu	-0.51	-0.32
AcAlaTyrLeuNH ₂	-0.04	-0.37

Therefore, for QikProp versions since 1.6, the log Po/w values for amino acids have been lowered by 2.0 log units, so that QikProp reproduces the Hansch * values. The correction is noted in the output files when it is applied.

Note that this correction is not just for the standard amino acids, but for any compound with a saturated amine group and a carboxylic acid, e.g., amoxicillin.

A similar correction factor is used by Hansch and Leo to account for zwitterions. They discuss this in [Ref. 15](#), and show that it works for molecules like amoxicillin which are zwitterionic.

1.3 Conformation Dependence of Results

The dependence of the QikProp results on molecular conformation has been studied by performing conformational searches on many molecules using BOSS with the OPLS-AA force field, followed by QikProp calculations for each conformer. The results demonstrate the following points:

1. There is generally modest difference in the QikProp predictions for different conformers. This results because the algorithms for determining the hydrogen-bond counts, which are very important descriptors, are independent of the 3D structure. The surface area and dipole moment terms are affected by conformation, but their variations are generally

small. The differences are always negligible for log BB and PCaco. The differences for log Po/w are also small, normally a few tenths of a log unit. The differences can be greater for log S, but rarely cover more than 1 log unit.

2. When there are differences, extended structures give results closer to the experimental data. The QikProp regressions have been developed using extended conformers; standard 2D–3D conversion programs usually generate extended conformers.
3. Boltzmann-weighting of the QikProp results using either the gas-phase conformer energies or the aqueous-phase conformer energies is probably not worth the effort, though it is theoretically desirable.

The results for six drugs are described below. The drugs each have multiple rotatable bonds, which were explored in the conformational searches. Clearly, negligible dependence of the results on conformation is expected for more rigid molecules.

- **acyclovir**—43 conformers covering an energy range of 9 kcal/mol were considered. The QPlogS values range from 0.3 to 0.5; the QPlogPo/w values range from –0.2 to –0.4.
- **epinephrine**—69 conformers covering an energy range of 14 kcal/mol were considered. The QPlogS values range from 0.3 to 0.6; the QPlogPo/w values range from –0.2 to –0.4.
- **haloperidol**—49 conformers covering an energy range of 18 kcal/mol were considered. The QPlogS values fall in two groups, –3 to –4 for very compact conformers with the fluorophenyl ring folded on top of the piperidine, and –4.5 to –5.0 for extended structures. The experimental log S is –4.4. The QPlogPo/w values range from 3.9 to 4.5 for all conformers.
- **linezolid**—68 conformers covering an energy range of 9 kcal/mol were considered. The QPlogS values range from –1.7 to –2.3; the QPlogPo/w values range from 0.3 to 0.9.
- **omeprazole**—42 conformers covering an energy range of 8 kcal/mol were considered. The QPlogS values range from –2.9 to –3.9 for the first 45 conformers; the QPlogPo/w values range from 1.5 to 2.2 for the first 42 conformers.
- **indinavir**—29 conformers covering an energy range of 8 kcal/mol were considered. The QPlogS values range from –2.3 to –0.2; the QP log Po/w values range from 0.8 to 1.4. This is a very flexible molecule with 16 variable dihedral angles included in the conformational search. The more extended structures give lower log S and higher log P values.

Statistical Analysis and Plots of Results

Plots of QikProp predictions against experiment are provided below. The sources of the experimental log P and log S values are described in Refs. 1, 2, and 3. Additional data has been kindly provided by Pharmacia Inc.

The databases of free energies of hydration and free energies of solvation in hexadecane are from Abraham et al [5].

The log BB values are mostly listed in Luco [6] and Kelder et al. [7]. The latter paper includes the experimental protocol. The values come from in vivo steady-state measurements using radiolabelled compounds with rats. The predicted CNS activities are based largely on log BB with some adjustments, and correspond well with the CNS activities reported in Table 1 of Ajay et al. [8].

The Caco-2 cell permeabilities are from Boehringer-Ingelheim (Yazdanian et al. [9] with minor additions), Affymax (Irvine et al. [10]), and Astra-Zeneca (Stenberg et al. [11]). The MDCK (Madin-Darby Canine Kidney) cell permeabilities are from the Affymax paper.

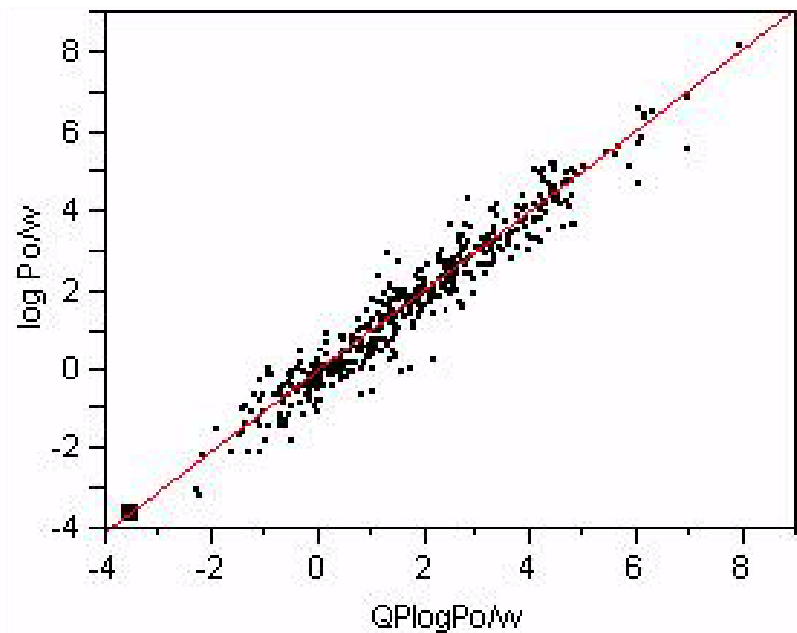
The experimental IC_{50} values for blockage of mammalian HERG K^+ channels are from Cavalli et al. [12], De Ponti et al. [13], and <http://www.fenichel.net>.

There is significant scatter in the experimental data amounting to uncertainties of factors of 2 to 50. The model has been based on all available data (47 compounds); however, this is still a small data set. Drugs that have been withdrawn owing to QT-prolongation problems also exhibit a large range of IC_{50} values, e.g., cisapride (6.5 nM), sertindole (14 nM), terfenadine (56 nM), and grepafloxacin (50000 nM). For trovafloxacin, the $Q\log HERG = -5$, so $IC_{50} = 10000$ nM. Thus, the allowable limit for IC_{50} values depends on the class of compounds, dosage, and bioavailability.

The log K_p values for skin permeability are from data of Flynn noted in Potts and Guy [14].

The log K_h data for binding to human serum albumin are from Colmenarejo et al. [4].

2.1 Octanol-Water Partition Coefficient, log P(o/w)



Linear Fit

$$\log P_{o/w} = -0.02883 + 1.0070235 \text{ QPlogPo/w}$$

Summary of Fit

RSquare	0.932266
RSquare Adj	0.932114
Root Mean Square Error	0.497341
Mean of Response	1.801786
Observations (or Sum Wgts)	448

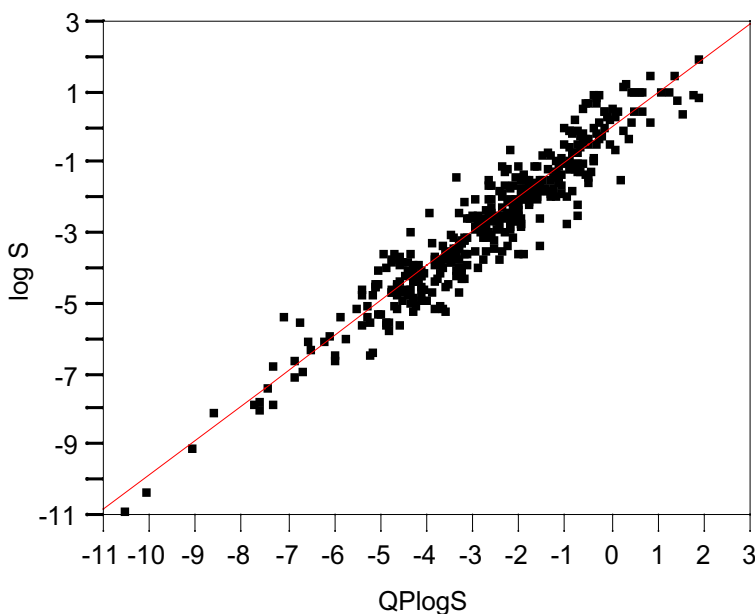
Analysis of Variance

Source	DF	Sum of Squares	Mean Square	F Ratio
Model	1	1518.3740	1518.37	6138.606
Error	446	110.3174	0.25	Prob > F
C. Total	447	1628.6914		<.0001

Parameter Estimates

Term	Estimate	Std Error	t Ratio	Prob> t
Intercept	-0.02883	0.033137	-0.87	0.3847
QPlogPo/w	1.0070235	0.012853	78.35	<.0001

2.2 Aqueous Solubility, log S



Linear Fit

$$\log S = 0.0235997 + 0.9849819 \text{ QPlogS}$$

Summary of Fit

RSquare	0.90504
RSquare Adj	0.904795
Root Mean Square Error	0.632696
Mean of Response	-2.60804
Observations (or Sum Wgts)	389

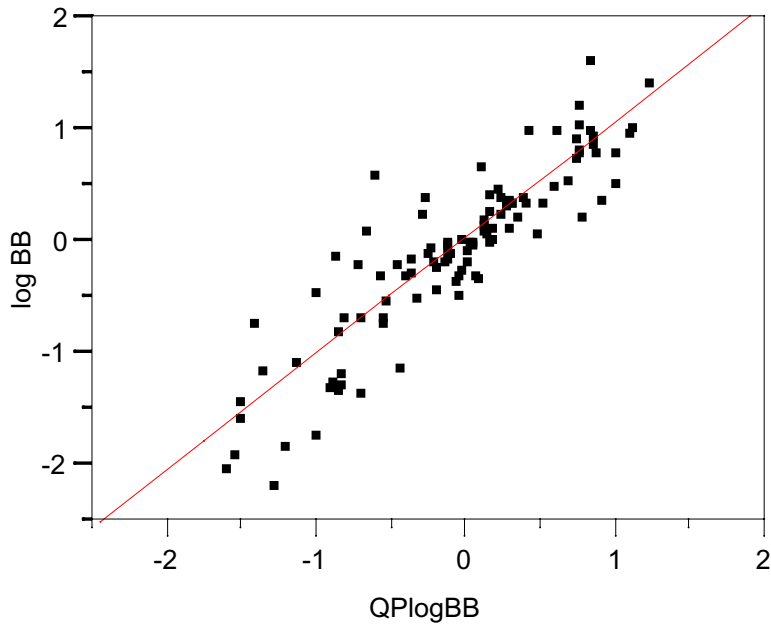
Analysis of Variance

Source	DF	Sum of Squares	Mean Square	F Ratio
Model	1	1476.4860	1476.49	3688.405
Error	387	154.9180	0.40	Prob > F
C. Total	388	1631.4040		<.0001

Parameter Estimates

Term	Estimate	Std Error	t Ratio	Prob> t
Intercept	0.0235997	0.053914	0.44	0.6618
QPlogS	0.9849819	0.016218	60.73	<.0001

2.3 Brain-Blood Partition Coefficient, log BB



Linear Fit

$$\log BB = 0.0177719 + 1.0311134 \text{ QPlogBB}$$

Summary of Fit

RSquare	0.802727
RSquare Adj	0.800793
Root Mean Square Error	0.349097
Mean of Response	-0.06644
Observations (or Sum Wgts)	104

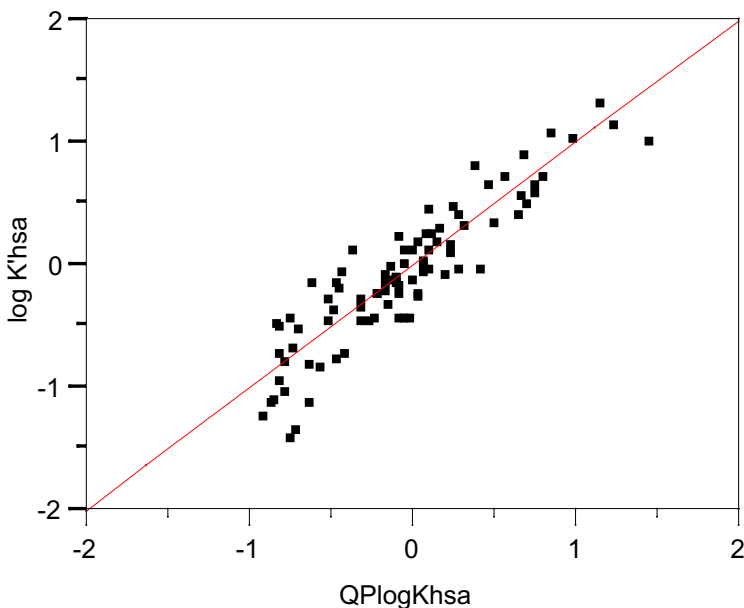
Analysis of Variance

Source	DF	Sum of Squares	Mean Square	F Ratio
Model	1	50.581700	50.5817	415.0512
Error	102	12.430596	0.1219	Prob > F
C. Total	103	63.012296		<.0001

Parameter Estimates

Term	Estimate	Std Error	t Ratio	Prob> t
Intercept	0.0177719	0.03448	0.52	0.6074
QPlogBB	1.0311134	0.050612	20.37	<.0001

2.4 Binding Affinity for Human Serum Albumin, log K'hsa



Summary of Fit

RSquare	0.82499
RSquare Adj	0.81005
Root Mean Square Error	0.252192
Mean of Response	-0.068
Observations (or Sum Wgts)	90

Analysis of Variance

Source	DF	Sum of Squares	Mean Square	F Ratio
Model	7	24.584558	3.51208	55.2205
Error	82	5.215282	0.06360	Prob > F
C. Total	89	29.799840		<.0001

Parameter Estimates

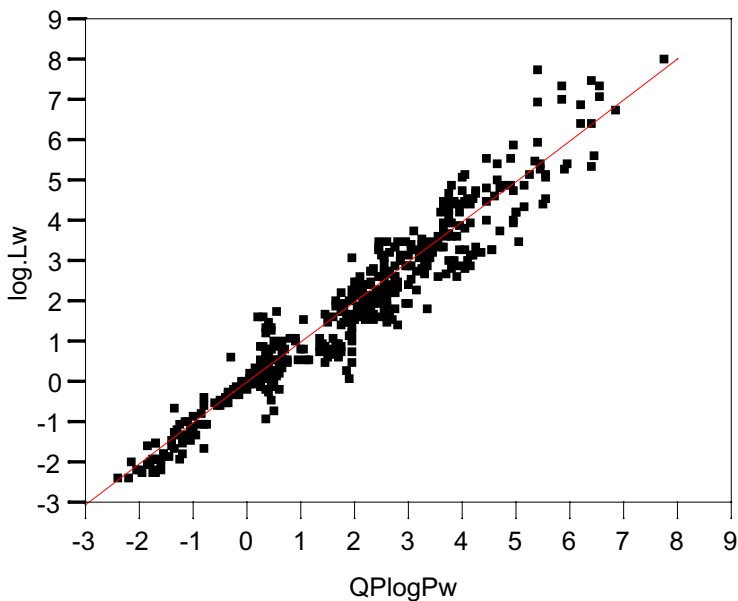
Term	Estimate	Std Error	t Ratio	Prob> t
Intercept	-1.538625	0.132628	-11.60	<.0001
volume	0.0031255	0.000225	13.89	<.0001
donorHB	-0.177019	0.05179	-3.42	0.0010
accptHB	-0.261692	0.026188	-9.99	<.0001
ACxDN^.5/SA	41.247956	9.920293	4.16	<.0001

Term	Estimate	Std Error	t Ratio	Prob> t
#acid	-0.163497	0.058579	-2.79	0.0065
#amide	-0.379871	0.06478	-5.86	<.0001
#rotor	-0.048244	0.013334	-3.62	0.0005

Effect Tests

Term	Nparm	DF	Sum of Squares	F Ratio	Prob>F
volume	1	1	12.275242	193.0039	<.0001
donorHB	1	1	0.743046	11.6829	0.0010
accptHB	1	1	6.351098	99.8585	<.0001
ACxDN ^{.5} /SA	1	1	1.099562	17.2884	<.0001
#acid	1	1	0.495440	7.7898	0.0065
#amide	1	1	2.187037	34.3868	<.0001
#rotor	1	1	0.832605	13.0911	0.0005

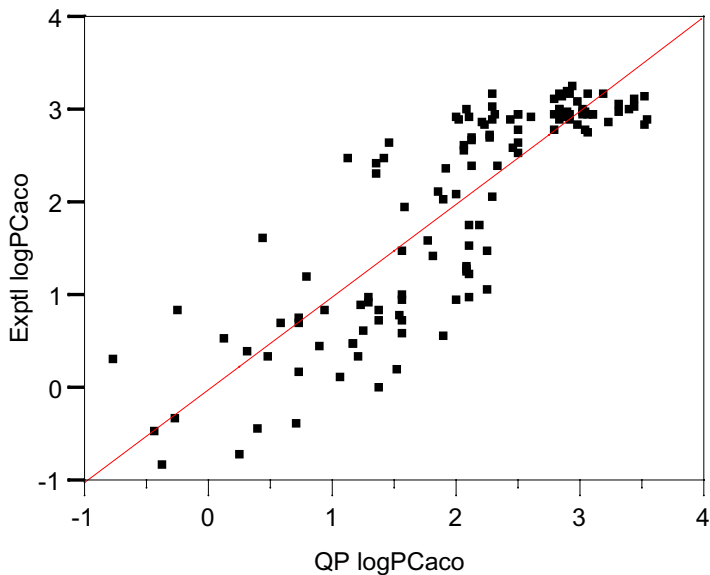
2.5 Free Energies of Hydration, $-2.3RT \log L_w$



Summary of Fit

RSquare	0.927252
RSquare Adj	0.927078
Root Mean Square Error	0.578191
Mean of Response	1.956532
Observations (or Sum Wgts)	421

2.6 Apparent Caco-2 cell permeability, log PCaco (Combined Data Sets)



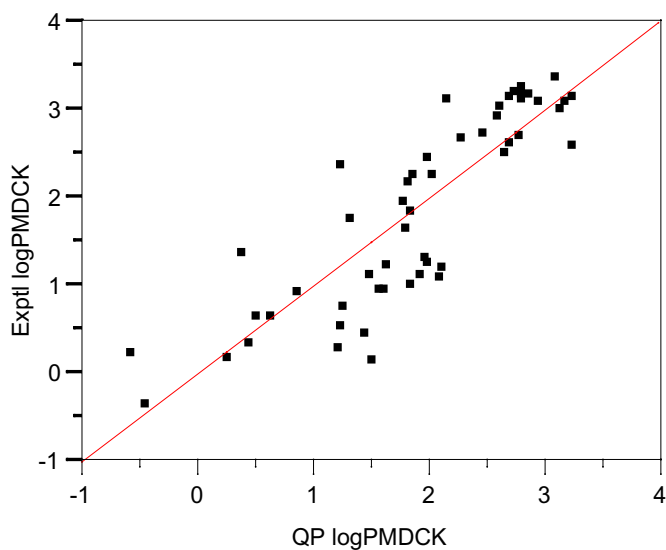
Linear Fit

$$\log\text{PCaco} = -0.000213 + 1.0000553 \text{ QPlogPCaco}$$

Summary of Fit

RSquare	0.717305
RSquare Adj	0.715025
Root Mean Square Error	0.608024
Mean of Response	1.999091
Observations (or Sum Wgts)	126

2.7 MDCK Cell Permeability, log PMDCK (Affymax Data)



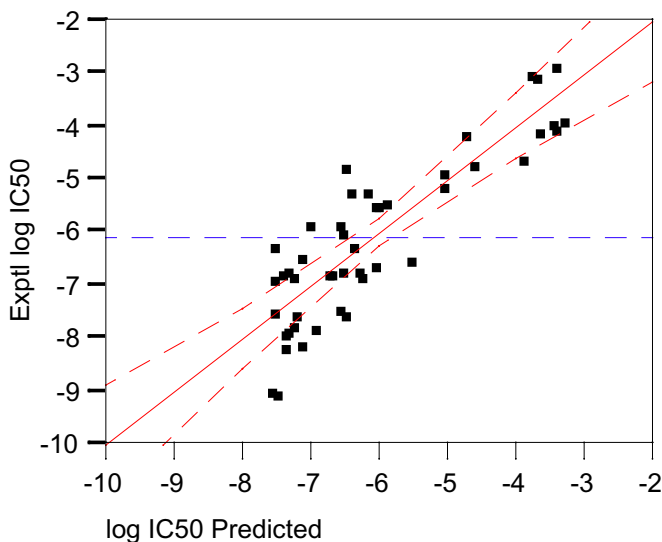
Linear Fit

$$\log\text{PMDCK} = -0.000825 + 1.0002359 \text{ QP logPMDCK}$$

Summary of Fit

RSquare	0.729367
RSquare Adj	0.723954
Root Mean Square Error	0.570739
Mean of Response	1.87335
Observations (or Sum Wgts)	52

2.8 Blockage of Mammalian HERG K⁺ Channels, log IC₅₀



Summary of Fit

RSquare	0.761105
RSquare Adj	0.738353
Root Mean Square Error	0.801461
Mean of Response	-6.09508
Observations (or Sum Wgts)	47

Analysis of Variance

Source	DF	Sum of Squares	Mean Square	F Ratio
Model	4	85.95097	21.4877	33.4523
Error	42	26.97827	0.6423	Prob > F
C. Total	46	112.92925		<.0001

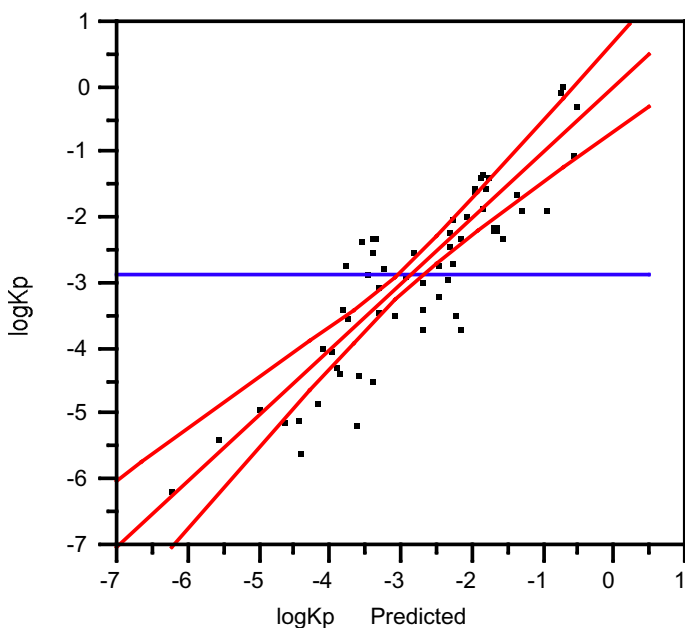
Parameter Estimates

Term	Estimate	Std Error	t Ratio	Prob> t
Intercept	-21.79849	2.744385	-7.94	<.0001
#acid	2.3543611	0.329979	7.13	<.0001
FOSA	0.0034346	0.000965	3.56	0.0009
#amide	2.7226498	0.582584	4.67	<.0001
glob	17.271181	3.289739	5.25	<.0001

Effect Tests

Source	Nparm	DF	Sum of Squares	F Ratio	Prob>F
#acid	1	1	32.699203	50.9064	<.0001
FOSA	1	1	8.134632	12.6641	0.0009
#amide	1	1	14.029161	21.8407	<.0001
glob	1	1	17.704597	27.5627	<.0001

2.9 Skin Permeability, log Kp



Summary of Fit

RSquare	0.779558
RSquare Adj	0.762921
Root Mean Square Error	0.678075
Mean of Response	-2.83707
Observations (or Sum Wgts)	58

Parameter Estimates

Term	Estimate	Std Error	t Ratio	Prob> t
Intercept	-1.519471	0.217782	-6.98	<.0001
#amine	-2.062598	0.266991	-7.73	<.0001
FISA	-0.01843	0.00183	-10.07	<.0001

Term	Estimate	Std Error	t Ratio	Prob> t
PISA	0.0035227	0.001012	3.48	0.0010
#rotor	0.096008	0.043569	2.20	0.0319

Effect Tests

Source	Nparm	DF	Sum of Squares	F Ratio	Prob>F
#amine	1	1	27.440404	59.6809	<.0001
FISA	1	1	46.611570	101.3767	<.0001
PISA	1	1	5.567049	12.1079	0.0010
#rotor	1	1	2.232640	4.8558	0.0319

References

1. Duffy, E. M.; Jorgensen, W. L. Prediction of Properties from Simulations: Free Energies of Solvation in Hexadecane, Octanol, and Water. *J. Am. Chem. Soc.* **2000**, *122*, 2878-2888.
2. Jorgensen, W. L.; Duffy, E. M. Prediction of Drug Solubility from Monte Carlo Simulations. *Bioorg. Med. Chem. Lett.* **2000**, *10*, 1155-1158.
3. Jorgensen, W. L.; Duffy, E. M. Prediction of Drug Solubility from Structure. *Adv. Drug Delivery Rev.* **2002**, *54*, 355-366.
4. Colmenarejo, G.; Alvarez-Pedraglio, A.; Lavandera, J.-L. Cheminformatic Models To Predict Binding Affinities to Human Serum Albumin. *J. Med. Chem.* **2001**, *44*, 4370-4378.
5. Abraham, M. H.; Andonian-Haftvan, J.; Whiting, G. S.; Leo, A.; Taft, R. S. *J. Chem. Soc. Perkin Trans.* **1994**, *2*, 1777-1791.
6. Luco, J. M. Prediction of the Brain-Blood Distribution of a Large Set of Drugs from Structurally Derived Descriptors Using Partial Least-Squares (PLS) Modeling. *J. Chem. Inf. Comput. Sci.* **1999**, *39*, 396-404.
7. Kelder J.; Grootenhuys, P. D. ;Bayada, D.M.; Delbressine, L.P., Ploemen, J.P. Polar molecular surface as a dominating determinant for oral absorption and brain penetration of drugs. *Pharm. Res.* **1999**, *16*, 1514-1519.
8. Ajay; Bemis, G. W.; Murkco, M. A. Designing Libraries with CNS Activity. *J. Med. Chem.*, **1999**, *42*, 4942-4951.
9. Yazdani M.; Glynn, S. L.; Wright, J. L.; Hawi A. Correlating partitioning and caco-2 cell permeability of structurally diverse small molecular weight compounds. *Pharm. Res.* **1998**, *15*, 1490-1494.
10. Irvine, J. D.; Takahashi, L.; Lockhart, K; Cheong, J.; Tolan, J. W.; Sclick, H. E.; Grove, J. R. MDCK (Madin-Darby canine kidney) cells: a tool for membrane permeability screening. *J. Pharm. Sci.* **1999**, *88*, 28-33.
11. Stenberg, P.; Norinder, U.; Luthman, K.; Artursson, P. Experimental and Computational Screening Models for the Prediction of Intestinal Drug Absorption. *J. Med. Chem.* **2001**, *44*, 1927-1937.

12. Cavalli, A.; Poluzzi, E.; De Ponti, F.; Recanatini, M. Toward a Pharmacophore for Drugs Inducing the Long QT Syndrome: Insights from a CoMFA Study of HERG K⁺ Channel Blockers *J. Med. Chem.* **2002**, *45*, 3844–3853.
13. De Ponti, F.; Poluzzi, E.; Montanaro, N. Organising evidence on QT prolongation and occurrence of Torsades de Pointes with non-antiarrhythmic drugs: a call for consensus. *Eur. J. Clin. Pharmacol.* **2001**, *57*, 185–209.
14. Potts, R. O.; Guy, R. H. Predicting skin permeability. *Pharm. Res.* **1992**, *9*, 663–669; A predictive algorithm for skin permeability: the effects of molecular size and hydrogen bond activity. *Pharm. Res.* **1995**, *12*, 1628–1633.
15. Exploring Qsar: Fundamentals and Applications in Chemistry and Biology; C Hansch, C.; Leo, A.; Hoekman, D. H., Eds.; Oxford University Press, 1995; p.156.

120 West 45th Street
32nd Floor
New York, NY 10036

101 SW Main Street
Suite 1300
Portland, OR 97204

3655 Nobel Drive
Suite 430
San Diego, CA 92122

Dynamostraße 13
68165 Mannheim
Germany

QuatroHouse, Frimley Road
Camberley GU16 7ER
United Kingdom

SCHRÖDINGER.